RESEARCH ARTICLE

Separations: Materials, Devices and Processes

Morphology prediction for organic molecular crystals using various force fields in ADDICT

Yongsheng Zhao[1] | Robert Gee[2] | Michael F. Doherty[1]

[1]Department of Chemical Engineering, University of California, Santa Barbara, California, USA

[2]Department of Computer Science, University of California, Santa Barbara, California, USA

Correspondence
Yongsheng Zhao and Michael F. Doherty, Department of Chemical Engineering, University of California Santa Barbara, Santa Barbara, CA 93106-5080, USA.
Email: yzhao01@ucsb.edu and mfd@ucsb.edu

Abstract

All-atom force fields are important for calculating interaction energies between growth units to predict crystal morphology. Our group at UCSB developed the ADDICT morphology design software to predict crystal morphology using mechanistic growth models driven by the generalized Amber force field (GAFF). In this study, the universal force field (UFF), the consistent force field (CFF), and the Coulomb-London-Pauli (CLP) force field are incorporated into ADDICT. We systematically test the lattice energies and crystal morphologies of olanzapine, adipic acid, rubrene, biphenyl, and naphthalene using all these force fields. The unit cells for these crystals are represented by the original CSD experimental structure, as well as optimized structures. Considering the high accuracy of CLP, its wide range of applications, and the fact that ADDICT can automatically specify the atomic charge and type required for this force field, we find that CLP is the best all-atom model to drive morphology calculations.

KEYWORDS
crystal growth, crystallization, design, solid-state physics

1 | INTRODUCTION

Crystal morphology plays a significant role in many industrial applications, with different crystal habits possessing different physical and chemical properties.[1–4] For example, designing crystals with a specific crystal face family can improve the catalytic activity of the crystal.[5] However, due to large number of crystalline substances, coupled with multiple growth conditions including solvent, additive, temperature, and supersaturation, it is a challenging task to obtain desired crystals with particular product functionality and morphology. In response, an academic design software called ADDICT (Advanced Design and Development of Industrial Crystallization Technology) was developed by our group at UCSB to predict crystal morphology.[1] One of the main goals of ADDICT is to model crystal growth and produce morphology outputs based on mechanistic growth models. In doing so, users can test different growth conditions such as solvent, supersaturation, and temperature to determine whether an improved morphology can be realized.

Recently, we upgraded ADDICT's software framework[6] and completely rewrote the code based on MATLAB using object-oriented programming in ADDICT3 (the third version of ADDICT).[7] The updated software framework of ADDICT3 includes three main parts: interpret crystallography, organize energetics, and implement mechanistic growth models.[6] Crystallography is a necessary input for the program. Before organizing energetics, the growth units with the lattice must be systematically organized and determined. At present, based on the new software framework, ADDICT3 can interpret the crystallography of varying types of crystals (including organic crystals, organic salts, solvates, and metal-organic crystals) with varying Z' (where Z' is the number of molecules in the asymmetric unit). With each growth unit in the unit cell defined, the solid-state interaction energy between growth units needs to be calculated. The interaction energy is the key to the mechanistic growth models. Its accuracy directly determines the quality of the predicted results. Different force fields may result in different interaction energies, which lead to different crystal morphologies. We previously used the generalized

Amber force field[8] (GAFF 1.8) as the default to calculate solid-state energy in ADDICT for organic crystals. Alternatives include the universal force field (UFF)[9] which is an all-atom potential that has parameters for every element from hydrogen to lawrencium. Although the results of UFF are sometimes not so accurate,[10] it is a force field for the entire periodic table, making it possible to predict the morphology of crystals containing atomic types not included in other force fields (e.g., metal-organic crystals). The Coulomb-London-Pauli (CLP)[11] is a force field specially developed for crystals. It can be used to predict the crystal morphology of most common organic crystals. In addition, the consistent force field (CFF)[12] (or Lifson force field) was developed specifically for carboxylic acid and amide crystals.

In this study, we first briefly introduce the GAFF, UFF, CLP, and CFF force fields. Then, we systematically study and compare the effect of those different force fields on the lattice energy and morphology of several crystals (e.g., olanzapine, adipic acid, rubrene, biphenyl, and naphthalene). In addition, we also discuss the effect of the optimization of the H atom positions on the lattice energy and crystal morphology.

2 | METHODOLOGY

2.1 | Generalized Amber force field

GAFF is currently one of the most popular all-atom force fields, which was developed by Wang et al.[8] In the previous version of ADDICT,[1] we used GAFF to calculate the solid-state interaction energy. Recently we have rewritten the GAFF code in an object-oriented language in ADDICT3 and set it as the default force field.[6,7] For a given i-j atom pair on different molecules, the intermolecular interaction (E_{ij}) is calculated using Equations (1)–(5). A_{ij} and B_{ij} are the Lennard-Jones parameters for repulsion and attraction, which can be calculated by mixing rules such as Lorentz-Berthelot mixing rules.[13] A_{ij} and B_{ij} can be expressed in terms of effective van der Waals radii and well depths, R_{ij}^* and ε_{ij} (Equations (2) and (3)), which can be further calculated from atomic parameters (Equations (4) and (5)). R_{ij} is the distance between atoms i and j; q_i and q_j are the partial charges for atoms i and j. The coulombic term represents interactions between the point charges q_i and q_j, and the default point charge for GAFF is the Restrained ElectroStatic Potential (RESP) charge.[14] Users need to use other software to calculate the RESP charge and provide it to ADDICT. For the van der Waals term, users also need to provide the atomic type for GAFF. For example, users can use Antechamber[15] to obtain mol2 files containing GAFF atomic charges and types.

$$E_{ij} = \frac{A_{ij}}{R_{ij}^{12}} - \frac{B_{ij}}{R_{ij}^6} + \frac{q_i q_j}{R_{ij}}, \tag{1}$$

$$A_{ij} = \varepsilon_{ij} \left(R_{ij}^* \right)^{12}, \tag{2}$$

$$B_{ij} = 2\varepsilon_{ij} \left(R_{ij}^* \right)^6, \tag{3}$$

$$R_{ij}^* = R_i^* + R_j^*, \tag{4}$$

$$\varepsilon_{ij} = \sqrt{\varepsilon_i \varepsilon_j}. \tag{5}$$

Based on the above equations, solid-state interactions between growth units can be calculated. Then we can predict the crystal morphology using mechanistic growth models based on molecular interaction energies, namely, kink energy, edge energy, and terrace energy.

2.2 | Universal force field

UFF is another popular all-atom force field, which was first proposed by Rappé et al.[9] The intermolecular interaction term of UFF is similar to Equation (1) of GAFF. The difference between UFF and GAFF is the way the van der Waals term is calculated.

$$E_{vdW} = D_{ij} \left\{ -2 \left[\frac{x_{ij}}{x} \right]^6 + \left[\frac{x_{ij}}{x} \right]^{12} \right\}, \tag{6}$$

where D_{ij} is the well depth (ε_{ij} in GAFF), x_{ij} is the van der Waals bond length, and x (R_{ij} in GAFF) is the distance between atoms i and j. Therefore, using the same notation as GAFF equation (6) can be rewritten as:

$$\begin{aligned} E_{vdW} &= -2\varepsilon_{ij} \left[\frac{x_{ij}}{R_{ij}} \right]^6 + \varepsilon_{ij} \left[\frac{x_{ij}}{R_{ij}} \right]^{12} \\ &= \frac{\varepsilon_{ij} x_{ij}^{12}}{R_{ij}^{12}} - \frac{2\varepsilon_{ij} x_{ij}^6}{R_{ij}^6} \\ &= \frac{A_{ij}}{R_{ij}^{12}} - \frac{B_{ij}}{R_{ij}^6} \end{aligned} \tag{7}$$

ε_{ij} in Equation (7) is calculated using Equation (5), and x_{ij} is calculated as:

$$x_{ij} = \sqrt{x_i x_j}, \tag{8}$$

where x_i and x_j are the van der Waals distances. It should be noted that although the UFF and GAFF equations both have the parameter well depth ε, they do not have all the same specific ε values because of their different ways of dividing atom types. This partial charge used by UFF is the charge equilibration (QEq). Like the GAFF force field, users also need to provide the QEq charge to ADDICT. However, users do not need to provide atomic types for UFF in ADDICT, because ADDICT can automatically assign them.

2.3 | CLP force field

The CLP force field was developed by Gavezzotti,[11] and has been principally parameterized to crystal lattice energies. This force field

includes four terms: Coulombic, polarization, dispersion (London), and repulsion (Pauli) terms. The default charge for CLP is estimated from a Mulliken population analysis on an Extended Hückel Theory[16] molecular orbital wavefunction. ADDICT automatically calculates this charge for CLP and also specifies the CLP atom type, so that users do not need to do any support calculations nor provide any charge input files. For a given atom pair on different growth units, the CLP interaction is calculated by:

$$E_{ij} = \frac{F_R T_{ij}}{R_{ij}^{12}} - \frac{F_D D_{ij}}{R_{ij}^6} - \frac{F_P P_{ij}}{R_{ij}^4} + \left(\frac{1}{4\pi\varepsilon^\circ}\right)\frac{q_i q_j}{R_{ij}}, \tag{9}$$

$$q_i = F_Q q_i^\circ. \tag{10}$$

R_{ij} is the internuclear distance between atoms i and j, q_i is the rescaled net charge on atom i, and F_Q, F_P, F_D, F_R are empirical scaling parameters. P, D, and T are coefficients calculated on the basis of the local environment of an atom in a given molecule:

$$\alpha_{\text{eff},i} = \alpha_i(Z_{V,i} - q_i)/Z_{V,i}, \tag{11}$$

$$\alpha_{i,j} = \left[(\alpha_{\text{eff},i})(\alpha_{\text{eff},j})\right]^{0.5}, \tag{12}$$

$$P_{i,j} = \alpha_{i,j}\text{abs}(q_i q_j), \tag{13}$$

$$D_{i,j} = \alpha_{i,j}n_i n_j (I_i I_j)^{0.5}, \tag{14}$$

$$T_{i,j} = (1 + H_{Bd}H_{Ba})(Z_{V,i} - q_i)(Z_{V,j} - q_j)(B_i B_j)^{0.5} \\ (\text{if } H_{Bd}H_{Ba} > 0, \text{then } H_{Bd}H_{Ba} = 0), \tag{15}$$

where α_i is the reference polarizability of atomic species, $Z_{V,i}$ is the number of valence electrons, n_i is the quantum number, I_i is the ionization potentials, B_i is an empirical "diffusion factor," and additional parameters H_{Bd} and H_{Ba} are hydrogen-bonding donor ability and acceptor ability, respectively. More details can be found in Gavezzotti's article.[11]

2.4 | Consistent force field

The consistent force field[12] (or Lifson force field) was mainly proposed for crystals containing intermolecular hydrogen bonds, such as carboxylic acid and amide crystals. The Lennard-Jones-Coulomb model is used in this force field with either 9 or 12 inverse powers for the repulsive term. The electrostatic term is the same as GAFF and UFF. In ADDICT, the following equation is used for CFF:

$$E_{ij} = \frac{A_{ij}}{R_{ij}^{12}} - \frac{B_{ij}}{R_{ij}^6} + \frac{q_i q_j}{R_{ij}}. \tag{16}$$

Although Equation (16) has the same expression as GAFF, the force field parameters of the van der Waals term of CFF are not the same as those of GAFF. The partial charge used by CFF is obtained by regression of calculated to experimental properties. Again, ADDICT can also automatically assign CFF atom types and partial charges.

2.5 | Mechanistic growth model

ADDICT3 incorporates mechanistic growth models (including spiral[17-19] and 2D-nucleation growth mechanisms[20]) into a new framework to predict the morphology of crystals using the solid-state interaction energy calculated from all-atom force fields.[6] If the growth rate of each face is known, the steady-state crystal morphology can be calculated using the Frank-Chernov construction:

$$\frac{G_1}{H_1} = \frac{G_2}{H_2} = \cdots = \frac{G_i}{H_i}, \tag{17}$$

where G_i is the perpendicular growth rate of face i, H_i is the perpendicular distance of face i from crystal center. The growth rate can be expressed as:

$$G = \frac{h}{\tau}, \tag{18}$$

where h is the interplanar spacing, and τ is the time taken to advance a face one layer. τ depends on the growth mechanism of the face. Considering that the crystals studied in this work are all under the spiral growth mechanism, here we only introduce the calculation of characteristic spiral rotation time. Spiral growth time τ is calculated by:

$$\tau = \sum_{i=1}^{N} \frac{l_{c,i+1}\sin(a_{i,i+1})}{v_i}, \tag{19}$$

where $\alpha_{i,i+1}$ is the angle between edge i and $i + 1$, $l_{c,i+1}$ is the critical length of edge $i + 1$, and v_i is the step velocity of edge i. The step velocity of the ith edge can be given by:

$$v_i = a_{p,i}\rho_i u_i, \tag{20}$$

where $a_{p,i}$ is the propagation length of edge i, u_i is the kink rate, and ρ_i is the kink density of kink sites of ith edge. The kink density and kink rate are obtained based on mechanistic energies (e.g., kink energies, edge energies, etc.) calculated from the all-atom force fields. More detailed information about the mechanistic growth theory and calculation process can be found elsewhere.[17-19,21]

2.6 | Crystal structure optimization

Accurate crystal structures are crucial for morphology prediction. The quality of the crystal structure depends on the expertise of the researchers and the nature of the experimental equipment. For example, hydrogen atoms are difficult to locate by X-ray so sometimes they

TABLE 1 Calculated lattice energy (kcal/mol) using four different force fields.

Crystal	GAFF	UFF	CLP	CFF	Exp.[a]
Olanzapine (CSD)	−35.306	−40.018	−39.306	o.s.	n.a.
Olanzapine (QM)	−33.466	−32.452	−36.940	o.s.	n.a.
Olanzapine (CLP)	−35.108	−32.476	−38.376	o.s.	n.a.
Adipic acid (CSD)	−42.814	+881.335	−29.092	−35.596	30.8[25]
Adipic acid (QM)	−34.621	+176.447	−29.844	−29.227	30.8[25]
Adipic acid (CLP)	−37.466	+215.675	−31.468	−31.096	30.8[25]
Rubrene (CSD)	−47.303	−70.663	−50.044	o.s.	44.0[26]
Rubrene (QM)	−45.709	−66.209	−48.029	o.s.	44.0[26]
Rubrene (CLP)	−46.037	−67.065	−48.397	o.s.	44.0[26]
Biphenyl (CSD)	−19.891	−28.390	−20.885	o.s.	19.9[25]
Biphenyl (QM)	−19.760	−27.643	−21.069	o.s.	19.9[25]
Biphenyl (CLP)	−19.748	−27.808	−21.033	o.s.	19.9[25]
Naphthalene (CSD)	−16.520	−23.889	−18.232	o.s.	18.2[25]
Naphthalene (QM)	−16.344	−22.772	−18.293	o.s.	18.2[25]
Naphthalene (CLP)	−17.300	−25.068	−18.310	o.s.	18.2[25]

Abbreviations: CLP, H atoms are geometrically optimized using the method in CLP-related paper; CSD, crystal structure is obtained from CSD; n.a., not available; o.s., outside scope of the model; QM, H atoms are optimized based on quantum method using Gaussian.
[a]Sublimation enthalpy (kcal/mol).

are assigned to incorrect positions or even missing in the structure files. Other times, duplicate atoms are reported in the structure files. Therefore, we need to optimize experimental crystal structures to initiate the morphology calculations with the best crystal structure file (cif file). In this work we leave all heavy atoms in their experimental positions and optimize the position of the hydrogen atoms only. There are two methods used in this work to optimize the H positions in cif files.

2.6.1 | QM-based method

Gaussian 09 software[22] can be used to optimize the positions of all hydrogen atoms (the positions of other atoms are fixed) using Becke's three-parameter function and Lee, Yang, and Parr's nonlocal correlation (B3LYP) together with the 6-31G* basis set.[23] Frequency analysis should also be performed at the same level of theory to ensure there are no imaginary frequencies and confirm the convergence (energy minimization).

2.6.2 | CLP-based method

ADDICT can geometrically optimize the positions of H atoms using Gavezzotti's method in the CLP-related paper.[11] In this method, the positions of H atoms are determined according to different atomic environments. For example, C−H hydrogens are optimized and reset by correcting CCH angles and at a distance of 1.08 Å from the connected C. Users only need to click a button in ADDICT to get a new optimized cif file.

3 | RESULTS AND DISCUSSION

3.1 | Lattice energy prediction using different force fields

To verify the accuracy of the different force fields, we compared the lattice energies calculated by ADDICT with the experimental sublimation energies. The lattice energy should be approximately equal to the negative experimental sublimation energy. Like Maloney et al.,[24] we assume that there are no intramolecular structural changes from solid state to gas phase.

We calculated the lattice energies of five crystals (olanzapine, adipic acid, rubrene, biphenyl, and naphthalene) under four different force fields (GAFF, UFF, CLP, and CFF). For each crystal we used the original CSD structure (CSD in parentheses in Table 1), the quantum method optimized structure (QM in parentheses in Table 1), and the CLP geometry-optimized structure (CLP in parentheses in Table 1).

As shown in Table 1, the lattice energies of olanzapine, rubrene, biphenyl, and naphthalene calculated by UFF are generally lower (more negative) than those calculated by other force fields and negative experimental sublimation energies. This shows that the lattice energy calculated by UFF is inaccurate or even wrong (for example, the lattice energy of adipic acid calculated by UFF is positive, which is obviously wrong because such a solid cannot be stable). The reason for the failure is that each element in the UFF force field has only one corresponding atomic type. For example, there is only one H atom type in UFF, while there are 8 and 13 types in CLP and GAFF, respectively. When the crystal has intermolecular hydrogen bonds like adipic acid, the problem with the UFF force field will be more prominent, and the calculated results will be unreliable. For example, as shown in
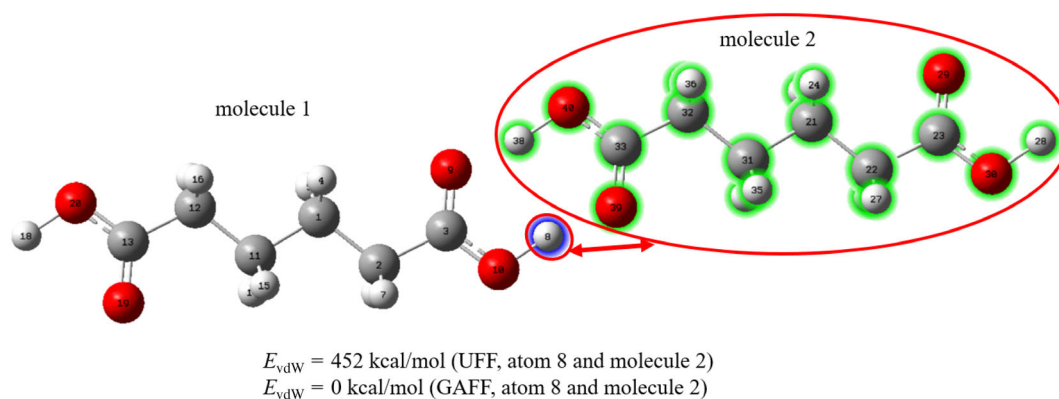
$E_{\text{vdW}} = 452$ kcal/mol (UFF, atom 8 and molecule 2)
$E_{\text{vdW}} = 0$ kcal/mol (GAFF, atom 8 and molecule 2)

FIGURE 1   van de Waals interaction between atom 8 of adipic acid molecule 1 and all atoms of molecule 2.

FIGURE 2   Morphology prediction of crystals olanzapine, adipic acid, rubrene, biphenyl, naphthalene using GAFF based on original structure reported in CSD (Original CSD), QM optimized structure (Optimized by QM), and geometrically optimized structure (Optimized by CLP). The CSD refcodes for the crystals used in this study are UNOGIN01 (olanzapine), ADIPAC (adipic acid), QQQCIG08 (rubrene), BIPHEN04 (biphenyl), and NAPHTA10 (naphthalene).

Figure 1, the van der Waals interaction between H atom 8 of adipic acid (original CSD structure) molecule 1 and all the atoms of molecule 2 is 452 kcal/mol obtained by UFF. However, it is 0 kcal/mol by GAFF.

The above results suggest that UFF may not be an ideal force field for predicting crystal morphology. The lattice energy for adipic acid calculated by CFF is in agreement with the experimental result and thus shows that it is suitable for the prediction of this crystal

TABLE 2 The predicted relative growth rates (R) using GAFF and corresponding colors of different face families for each of the crystals in Figure 2.

Crystal	Family	R (CSD)	R (QM)	R (CLP)	Color
Olanzapine	{1 0 0}	1	1	1	Blue
	{0 1 1}	3.14	3.06	3.19	Red
Adipic acid	{0 1 1}	1	1	1	Yellow
	{1 0 0}	100	100	100	Blue[a]
Rubrene	{2 0 0}	1	1	1	Blue
	{0 0 2}	1.80	2.10	2.04	Red
	{1 1 1}	27.89	12.20	13.15	Pink[a]
Biphenyl	{0 0 1}	1	1	1	Blue
	{1 1 0}	2.54	2.56	2.61	Green
Naphthalene	{0 0 1}	1	1	1	Blue
	{1 1 0}	2.77	2.85	3.27	Pink
	{1 1 1}	2.86	2.95	3.38	Red
	{2 0 1}	3.63	3.85	3.49	Yellow

[a]The face family with the smallest area.

morphology. However, CFF cannot be used for the other cases in Table 1, thus limiting the application of this force field. Except for adipic acid, the lattice energies of other crystals calculated by CLP and GAFF are relatively close to each other as well as the experimental results, indicating that both of them are good candidates for morphology predictions of those crystals. In addition, the lattice energy of adipic acid (CSD) calculated by GAFF is −42.814 kcal/mol, which is significantly different from the experimental value, suggesting that it is necessary to optimize the crystal structure. For some crystals such as biphenyl, the lattice energy of the optimized structure is close to that before optimization, indicating that they are expected to have very similar crystal morphologies, so optimization of this crystal was not necessary. To isolate the effect of force field we study the morphology of crystals grown from the vapor. The energy interactions between growth units for such crystals do not need to be modified by the effect of solvent—thereby eliminating any "contamination" by solvent models on our results. Thus, the atom-atom force fields used to calculate the values in Table 1 are the only energy models used to drive the morphology predictions.

3.2 | Morphology prediction using GAFF

As shown in Figure 2, we predicted the crystal morphologies for olanzapine (Figure 2A–C), adipic acid (Figure 2D–F), rubrene (Figure 2G–I), biphenyl (Figure 2J–L), and naphthalene (Figure 2M–O) grown from vapor (sublimation growth) using GAFF in ADDICT based on the original structure file from CSD (Original CSD), QM optimized structure (Optimized by QM), and geometrically optimized structure (Optimized by CLP), respectively. The detailed relative growth rates of different face families for the above crystals can be found in Table 2.

The experimental and previous predicted crystal morphologies of these crystals can be found in Figure 3 (the experimental sublimation morphology for olanzapine is not available). Those crystal morphologies for rubrene and naphthalene obtained with GAFF are in good agreement with the experiments. For biphenyl, the slowest face family {0 0 1} is correctly predicted. Of the surrounding indexed faces, the {1 1 0} face family is indeed predicted, while the {1 0 0} face family grows out of the predicted steady-state shape. The {2 1 0} face family has only 1 single periodic bond chain (S face), so one would not expect it to appear on the steady-state crystal shape. The imaged crystal is asymmetric, which should not be the case for unhindered growth of a nonpolar crystal.[25] It is possible that the experimental habit is not the steady-state habit but instead a habit obtained prior to steady-state. For adipic acid, the original crystal structure from CSD has the lowest lattice energy, but it is quite different from the experimental value, which means that this crystal structure needs to be optimized. The predicted crystal morphology of adipic acid based on the optimized structures are still not perfect, indicating that GAFF may not be well suited for this crystal. There is a mismatch of Miller indices for adipic acid between the faces predicted and those indexed experimentally. This could be a result of the small face areas available for indexing.[25] In addition to the fact that faces with high Miller indices are less likely to occur, one would also not expect corresponding places on the crystal shape to have different face families (e.g., {0 0 1} and {3 −1 −6}). In addition, it can be seen from Figure 2 and Table 1 that when the lattice energies calculated based on different crystal structures are close to each other, the morphologies of the crystals are also similar to each other (the growth rates of the crystal faces are close to each other too, see Table 2).

3.3 | Morphology prediction using UFF

The predicted crystal morphologies for olanzapine (Figure 4A–C), rubrene (Figure 4D–F), biphenyl (Figure 4G–I), and naphthalene (Figure 4J–L) grown from vapor using UFF based on the original CSD structure and optimized structures are provided in Figure 4. The detailed relative growth rates of different face families for the above crystals can be found in Table 3. Since the lattice energy of adipic acid calculated by UFF is positive we could not use UFF to predict the morphology of this crystal. The predicted crystal morphology of naphthalene based on the CLP geometry optimized structure is closest to the experimental structure in Figure 3. The predicted crystal morphologies based on the three different structures of biphenyl (Figure 4G–I) are very close to each other because their lattice energies are very close, leading to similar relative growth rates of their different faces (see Table 3). Although UFF can accurately predict the Miller indices and the slowest growth face for rubrene, UFF does not work well for predicting the morphology of this crystal because its lattice energies differ greatly from the experimental value. The predicted morphologies of olanzapine using UFF are not good, and the slowest growth face is not the same as GAFF and our previous work.[17]
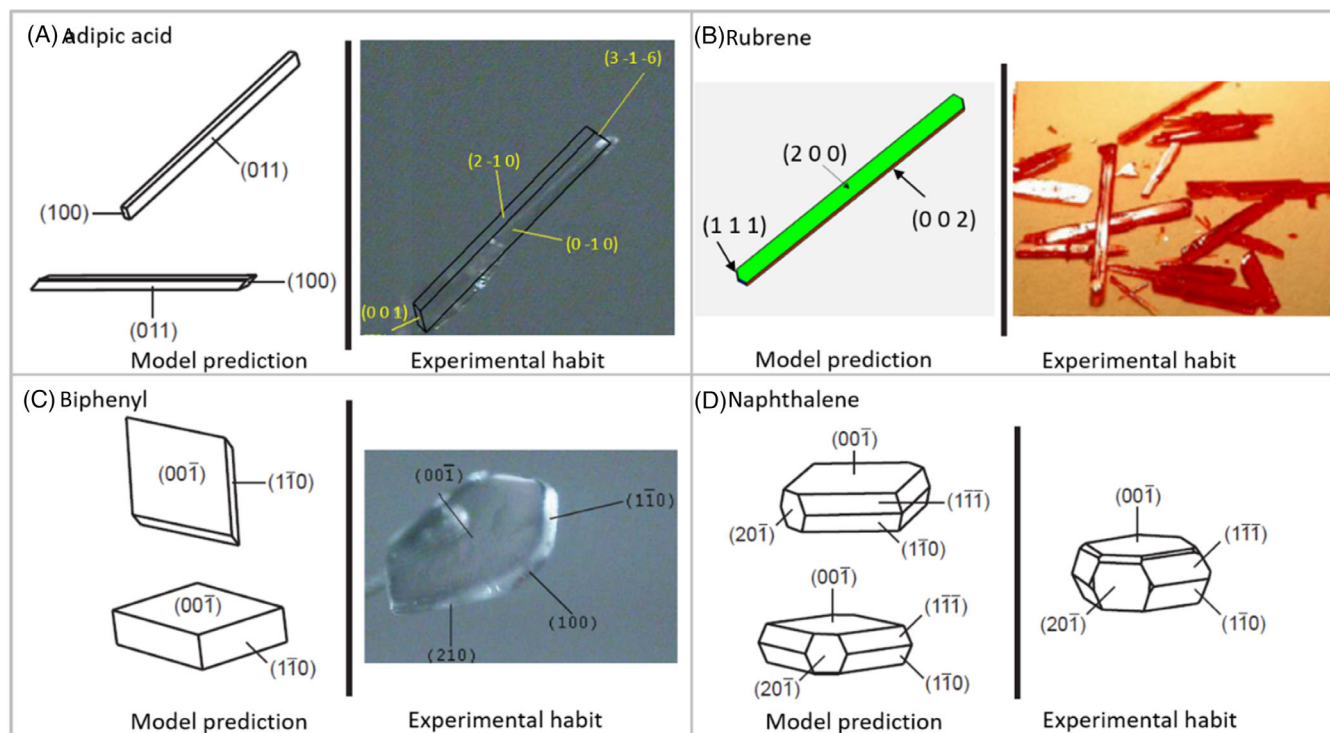
FIGURE 3 Previous predicted morphologies based on spiral growth model and experimental morphologies for (A) adipic acid,[25] (B) rubrene,[7,27] (C) biphenyl,[25] and (D) naphthalene[25,28] grown from vapor.
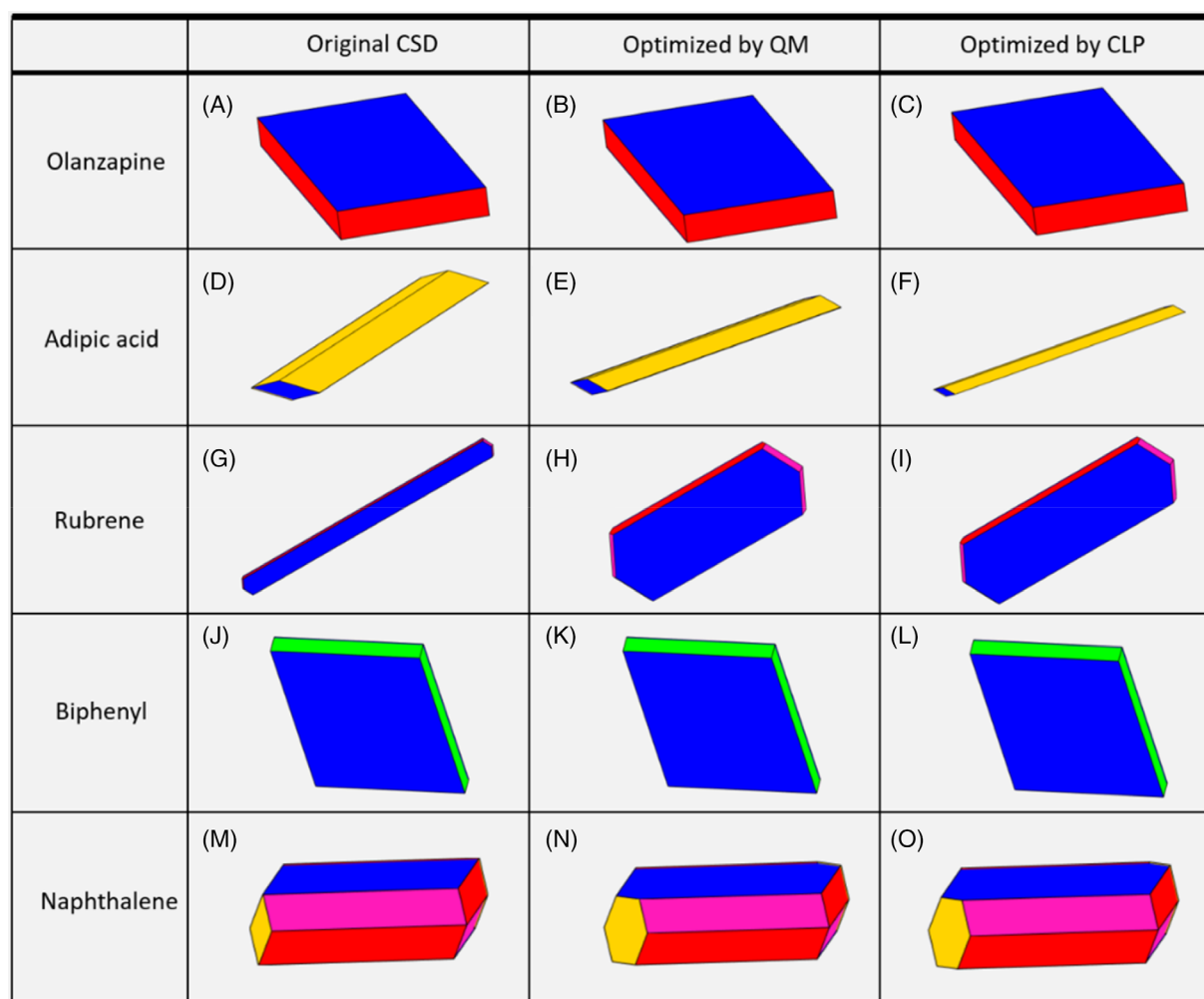

FIGURE 4 Morphology prediction of crystals olanzapine, rubrene, biphenyl, naphthalene using UFF based on original structure reported in CSD (Original CSD), QM optimized structure (Optimized by QM), and geometrically optimized structure (Optimized by CLP). The CSD refcodes are the same as in Figure 2.

TABLE 3 The predicted relative growth rates (R) using UFF and corresponding colors of different face families for different crystals in Figure 4.

Crystal	Family	R (CSD)	R (QM)	R (CLP)	Color
Olanzapine	{1 0 0}	12.96	76.52	100	Blue
	{0 1 1}	1.12	2.19	2.29	Red
	{0 2 0}	1	1	1	Pink
Rubrene	{2 0 0}	1	1	1	Blue
	{0 0 2}	1.61	1.66	1.62	Red
	{1 1 1}	100	100	100	Pink[a]
Biphenyl	{0 0 1}	1	1	1	Blue
	{1 1 0}	2.98	2.79	2.83	Green
Naphthalene	{0 0 1}	1	1	1	Blue
	{1 1 0}	2.72	2.95	3.47	Pink
	{1 1 1}	2.81	3.05	3.58	Red
	{2 0 1}	5.99	5.00	4.90	Yellow

[a]The face family with the smallest area.

TABLE 4 The predicted relative growth rates (R) using CLP and corresponding colors of different face families for each of the crystals in Figure 5.

Crystal	Family	R (CSD)	R (QM)	R (CLP)	Color
Olanzapine	{1 0 0}	1	1	1	Blue
	{0 1 1}	2.87	3.01	3.00	Red
Adipic acid	{0 1 1}	1	1	1	Yellow
	{1 0 0}	4.46	9.45	16.28	Blue
Rubrene	{2 0 0}	1	1	1	Blue
	{0 0 2}	1.81	2.72	2.48	Red
	{1 1 1}	23.80	6.63	7.48	Pink[a]
Biphenyl	{0 0 1}	1	1	1	Blue
	{1 1 0}	2.65	2.66	2.64	Green
Naphthalene	{0 0 1}	1	1	1	Blue
	{1 1 0}	2.84	3.18	3.12	Pink
	{1 1 1}	2.93	3.29	3.22	Red
	{2 0 1}	4.58	4.57	4.53	Yellow

[a]The face family with the smallest area.

FIGURE 5 Morphology prediction of crystals olanzapine, adipic acid, rubrene, biphenyl, naphthalene using CLP based on original structure reported in CSD (Original CSD), QM optimized structure (Optimized by QM), and geometrically optimized structure (Optimized by CLP). The CSD refcodes are the same as in Figure 2.
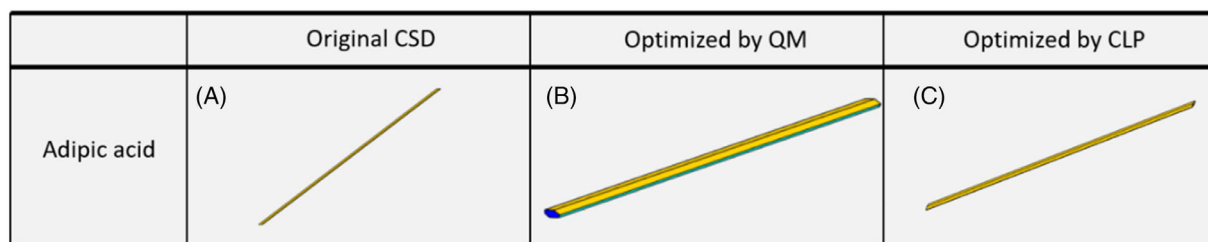
FIGURE 6 Morphology prediction of adipic acid using CFF based on original structure form CSD (Original CSD), QM optimized structure (Optimized by QM), and geometrically optimized structure (Optimized by CLP). The CSD refcode is the same as in Figure 2.

TABLE 5 The predicted relative growth rates (*R*) using CFF and corresponding colors of different face families for adipic acid in Figure 6.

Crystal	Family	R (CSD)	R (QM)	R (CLP)	Color
Adipic acid	{0 1 1}	1	1	1	Yellow
	{0 0 2}	1.11	1.05	1.15	Cyan
	{1 0 0}	100	19.69	60.09	Blue[a]

[a]The face family with the smallest area.

TABLE 6 Summary and comparison of GAFF, UFF, CLP, and CFF force fields in ADDICT.

Force field	Number of atom type	Application range	Accuracy[a]	Software needed for atom charge and type
GAFF	71 (Sometimes one element corresponds to multiple types)	Wide range	Very good/good	Gaussian, Antechamber, or others
UFF	103 (one element corresponds to one type)	The widest range	Not so good (especially for H-bond crystals)	Gaussian or others for QEq charge
CLP	60 (Sometimes one element corresponds to multiple types)	Wide range	Very good	No need
CFF	9 (including C, H, O, and N four elements)	Limited range	Very good for corresponding crystals	No need

[a]The accuracy is obtained based on the best results of three different structures.

3.4 | Morphology prediction using CLP

It can be seen from Figures 3 and 5 that the predicted crystal morphologies based on CLP are in good agreement with the experimental results. The detailed relative growth rates for each face family and each crystal structure predicted by CLP can be found in Table 4. Compared with the results predicted by GAFF and UFF, the crystal morphology predicted by CLP for adipic acid is better. The predicted relative growth rates for {1 0 0} face family of adipic acid (see Table 4) based on three different structures are 4.46, 9.45, and 16.28, respectively. However, the growth rates for the {1 0 0} face family of adipic acid calculated by GAFF are much greater than these values. This explains why the predicted crystal morphology of adipic acid based on GAFF is needle-shaped, while that predicted based on CLP is a rod.

As can be seen from Figure 5, Tables 1 and 4, since the lattice energies of different structures of the same crystal calculated by CLP are relatively close to each other, these structures of the same crystal have similar relative growth rates and crystal morphologies. In addition, we can see that the lattice energies of rubrene based on the original CSD structure calculated by GAFF, UFF, and CLP are close to the

other two optimized structures, which may imply that no optimization is needed for this crystal. We can obtain good morphology prediction for rubrene based on the original CSD structure.

3.5 | Morphology prediction using CFF

Since the CFF (Lifson) force field was developed for crystals of carboxylic acids and amides, its application range is limited. Therefore, CFF can only be used to predict the crystal morphology of one of the five crystals studied in this article, that is, adipic acid. The predicted crystal morphologies based on the three different structures using CFF are shown in Figure 6, and the corresponding relative growth rates of face families are shown in Table 5. The predicted crystal lattice energies and morphologies based on the optimized structures are better than the predictions based on the original CSD structure. It should be pointed out that the atomic charges corresponding to the three crystal structures of adipic acid are the same because we used the charges obtained by the CFF force field regression. Given that the three structures are somewhat different, it is not very reasonable to

assign them exactly equal charges. Since the van der Waals parameters and charges in the CFF force field were obtained in the original source paper based on the optimized structure,[12] we recommend the optimized structures when using the CFF force field.

3.6 | Comparison of GAFF, UFF, CLP, and CFF

A summary and comparison of the GAFF, UFF, CLP, and CFF force fields based on the five crystals studied in this article are provided in Table 6. GAFF, UFF, and CLP contain many atom types and thus can be used for a wide range of applications. GAFF and CLP can be used for most common organic crystals. UFF can be even used for metal crystals. GAFF and CLP are generally more accurate than UFF predictions, especially for crystals containing intermolecular hydrogen bonds. Although the CFF force field contains fewer atom types than other force fields, limiting its application, it has good prediction results for crystals in the range of its application. For the GAFF force field, we need to use Gaussian and Antechamber (or other software) to get the atomic types and associated atomic RESP charges. For the UFF force field, we need Gaussian (or other software) to get the QEq charge. However, we wrote code in ADDICT to specify the atomic types of CLP and CFF and get the corresponding atomic charges, so users can run them directly to test their crystals without using other software. After comprehensive consideration, we determined that the CLP force field is the best one available for general purpose morphology prediction for organic crystals.

4 | CONCLUSIONS

Different force fields may result in different interaction energies, which lead to different crystal morphologies. Therefore, it is necessary to systematically study the effect of different force fields on the crystal morphology. In this study, we have investigated the lattice energies of olanzapine, adipic acid, rubrene, biphenyl, and naphthalene (including experimental and optimized crystal structures) using four force fields: GAFF, UFF, CLP, and CFF. We then investigated their predicted crystal morphologies using mechanistic growth models in ADDICT. By comparison and analysis, we recommend using CLP as the default force field to predict the morphologies of common organic crystals. We can determine whether the crystal structure needs to be optimized by comparing how close the predicted lattice energies are to the experimental sublimation enthalpy.

DATA AVAILABILITY STATEMENT
Data available on request from the authors.

ORCID
Yongsheng Zhao https://orcid.org/0000-0003-1224-1787

REFERENCES
1. Li J, Tilbury CJ, Kim SH, Doherty MF. A design aid for crystal growth engineering. *Prog Mater Sci*. 2016;82:1-38.
2. de Albuquerque I, Mazzotti M, Ochsenbein DR, Morari M. Effect of needle-like crystal shape on measured particle size distributions. *AIChE J*. 2016;62(9):2974-2985.
3. Ramamoorthy S, Kwak JH, Karande P, Farmanesh S, Rimer JD. A high-throughput assay for screening modifiers of calcium oxalate crystallization. *AIChE J*. 2016;62(10):3538-3546.
4. Chai S, Li E, Zhang L, Du J, Meng Q. Crystallization solvent design based on a new quantitative prediction model of crystal morphology. *AIChE J*. 2022;68(1):e17499.
5. Yang HG, Sun CH, Qiao SZ, et al. Anatase TiO2 single crystals with a large percentage of reactive facets. *Nature*. 2008;453(7195):638-641.
6. Zhao Y, Tilbury CJ, Landis S, et al. A new software framework for implementing crystal growth models to materials of any crystallographic complexity. *Cryst Growth Des*. 2020;20(5):2885-2892.
7. Landis S, Zhao Y, Doherty MF. Digital design of crystalline solids. *Comput Chem Eng*. 2020;133:106637.
8. Wang J, Wolf RM, Caldwell JW, Kollman PA, Case DA. Development and testing of a general amber force field. *J Comput Chem*. 2004;25(9):1157-1174.
9. Rappé AK, Casewit CJ, Colwell K, Goddard WA III, Skiff WM. UFF, a full periodic table force field for molecular mechanics and molecular dynamics simulations. *J Am Chem Soc*. 1992;114(25):10024-10035.
10. Martin MG. Comparison of the AMBER, CHARMM, COMPASS, GROMOS, OPLS, TraPPE and UFF force fields for prediction of vapor–liquid coexistence curves and liquid densities. *Fluid Phase Equilib*. 2006;248(1):50-55.
11. Gavezzotti A. Efficient computer modeling of organic materials. The atom–atom, Coulomb–London–Pauli (AA-CLP) model for intermolecular electrostatic-polarization, dispersion and repulsion energies. *New J Chem*. 2011;35(7):1360-1368.
12. Lifson S, Hagler A, Dauber P. Consistent force field studies of intermolecular forces in hydrogen-bonded crystals. 1. Carboxylic acids, amides, and the C:O. cntdot..cntdot..cntdot. H-hydrogen bonds. *J Am Chem Soc*. 1979;101(18):5111-5121.
13. Wang J, Cieplak P, Li J, et al. Development of polarizable models for molecular mechanical calculations. 4. Van der Waals parametrization. *J Phys Chem B*. 2012;116(24):7088-7101.
14. Bayly CI, Cieplak P, Cornell W, Kollman PA. A well-behaved electrostatic potential based method using charge restraints for deriving atomic charges: the RESP model. *J Phys Chem*. 1993;97(40):10269-10280.
15. Wang J, Wang W, Kollman PA, Case DA. Automatic atom type and bond type perception in molecular mechanical calculations. *J Mol Graph Model*. 2006;25(2):247-260.
16. Hoffmann R. An extended Hückel theory. I. Hydrocarbons. *J Chem Phys*. 1963;39(6):1397-1412.

17. Snyder RC, Doherty MF. Predicting crystal growth by spiral motion. *Proc R Soc A: Math Phys Eng Sci*. 2009;465(2104):1145-1171.

18. Kuvadia ZB, Doherty MF. Spiral growth model for faceted crystals of non-centrosymmetric organic molecules grown from solution. *Cryst Growth Des*. 2011;11(7):2780-2802.

19. Tilbury CJ, Doherty MF. Modeling layered crystal growth at increasing supersaturation by connecting growth regimes. *AIChE J*. 2017; 63(4):1338-1352.

20. Lovette MA, Doherty MF. Predictive modeling of supersaturation-dependent crystal shapes. *Cryst Growth Des*. 2012;12(2):656-669.

21. Sun Y, Tilbury CJ, Reutzel-Edens SM, Bhardwaj RM, Li J, Doherty MF. Modeling olanzapine solution growth morphologies. *Cryst Growth Des*. 2018;18(2):905-911.

22. Frisch M, Trucks G, Schlegel H, et al. *Gaussian 09, Revision D.01*. Gaussian Inc.; 2009.

23. Ditchfield R, Hehre WJ, Pople JA. Self-consistent molecular-orbital methods. IX. An extended gaussian-type basis for molecular-orbital studies of organic molecules. *J Chem Phys*. 1971;54(2):724-728.

24. Maloney AG, Wood PA, Parsons S. Intermolecular interaction energies in transition metal coordination compounds. *CrystEngComm*. 2015;17(48):9300-9310.

25. Tilbury CJ, Green DA, Marshall WJ, Doherty MF. Predicting the effect of solvent on the crystal habit of small organic molecules. *Cryst Growth Des*. 2016;16(5):2590-2604.

26. Lima CF, Costa JC, Lima LMSS, Melo A, Silva AM, Santos LM. Energetic and structural insights into the molecular and supramolecular properties of rubrene. *ChemistrySelect*. 2017;2(5):1759-1769.

27. de Boer RWI, Gershenson M, Morpurgo A, Podzorov V. Organic single-crystal field-effect transistors. *Phys Status Solidi A*. 2004; 201(6):1302-1331.

28. Grimbergen R, Reedijk M, Meekes H, Bennema P. Growth behavior of crystal faces containing symmetry-related connected nets: a case study of naphthalene and anthracene. *J Phys Chem B*. 1998;102(15):2646-2653.